The current issue and full text archive of this journal is available at
www.emeraldinsight.com/0961-5539.htm

Buoyancy effects on upward and downward laminar mixed convection heat and mass transfer in a vertical channel

Received 1 January 2006
Accepted 9 July 2006

Youssef Azizi and Brahim Benhamou
LMFE, Physics Department, Faculty of Sciences Semlalia, Marrakech, Morocco
Nicolas Galanis
THERMAUS, Département de génie mécanique, Université de Sherbrooke, Québec, Canada, and
Mohammed El-Ganaoui
SPCTS, Département de Physique, Faculté des Sciences et Techniques, Limoges, France

Abstract

Purpose – The objective of the present study is to investigate numerically the effects of thermal and buoyancy forces on both upward flow (UF) and downward flow (DF) of air in a vertical parallel-plates channel. The plates are wetted by a thin liquid water film and maintained at a constant temperature lower than that of the air entering the channel.

Design/methodology/approach – The solution of the elliptical PDE modeling the flow field is based on the finite volume method.

Findings – Results show that buoyancy forces have an important effect on heat and mass transfers. Cases with evaporation and condensation have been investigated for both UF and DF. It has been established that the heat transfer associated with these phase changes (i.e. latent heat transfer) may be more or less important compared with sensible heat transfer. The importance of these transfers depends on the temperature and humidity conditions. On the other hand, flow reversal has been predicted for an UF with a relatively high temperature difference between the incoming air and the walls.

Originality/value – Contrary to most studies in channel heat and mass transfer with phase change, the mathematical model considers the full elliptical Navier-Stokes equations. This allows one to compute situations of flow reversal.

Keywords Heat transfer, Convection, Flow measurement

Paper type Research paper

Nomenclature

b = channel width (m)
C = dimensionless mass fraction, $= (w - w_0)/(w_w - w_0)$
D = mass diffusion coefficient (m s^{-2})
D_h = hydraulic diameter, $= 2b$ (m)
f = friction factor
g = gravitational acceleration (m s^{-2})
Gr_M = solutal Grashof number, $= g\beta^* D_h^3 (w_w - w_0)/\nu^2$
Gr_T = thermal Grashof number, $= g\beta D_h^3 (T_w - T_0)/\nu^2$
Gr^+ = effective Grashof number, $= Gr_T + Gr_M$
h_{fg} = latent heat of vaporization/

International Journal of Numerical Methods for Heat & Fluid Flow
Vol. 17 No. 3, 2007
pp. 333-353

0961-5539
DOI 10.1108/09615530710730193

condensation (J kg^{-1})
k = thermal conductivity (W m^{-1} K^{-1})
L = channel height (m)
M_a = molecular mass of air (kg $kmol^{-1}$)
M_v = molecular mass of water vapor (kg $kmol^{-1}$)
Nu_S = local Nusselt number for sensible heat transfer
Nu_L = local Nusselt number for latent heat transfer
P_m = dimensionless pressure, $= (p - \rho_0 gx)/\rho_0 U_0^2$
Pr = Prandtl number
q = heat flux (W m^{-2})
Re = Reynolds number, $= U_0 D_h/\nu$
Sc = Schmidt number, $= \nu/D$
Sh = Sherwood number
T = temperature (K)
U, V = dimensionless velocity components
V_e = dimensionless transverse vapor velocity
W = mass fraction ((kg of vapor) (kg of mixture)$^{-1}$)
x, y = axial and transverse co-ordinates (m)
X, Y = dimensionless co-ordinates

Greek symbols
β = coefficient of thermal expansion, $= 1/T_0$ (K^{-1})
β^* = coefficient of mass fraction expansion, $= M_a/M_v - 1$
γ = aspect ratio of the channel, $= b/L$
θ = dimensionless temperature, $= (T - T_0)/(T_w - T_0)$
ν = kinematic viscosity (m^2 s^{-1})
ρ = density (kg m^{-3})
ϕ = relative humidity (%)

Subscripts
0 = at the inlet
m = mean value
w = at the wall
L = relative to latent heat transfer
S = relative to sensible heat transfer

1. Introduction

Engineering applications of confined flows with simultaneous thermal and mass diffusion are many. Cooling of electronic equipment, desalination, cooling towers and air conditioning (i.e. evaporative cooling) are some of these applications.

Many analyses of combined heat and mass transfer convection in channels are available in the literature. Nelson and Wood (1989) studied a developing laminar natural convection flow in a vertical parallel-plates channel. They used a boundary-layer approximation model to derive a correlation for heat and mass transfer coefficients in the case of uniform temperature and concentration plates. Yan and Lin (1990) analyzed the effect of latent heat transfer of finite liquid film wetting the channel walls on laminar natural convection heat and mass transfer. They considered uniform temperature walls wetted with ethanol or water films. Their numerical study concluded that the assumption of extremely thin film is valid when the liquid mass flow rate is small. The same result was obtained for downward laminar mixed convection in the case of uniform wall heat flux by Yan (1992) and in the case of uniform wall temperature by Yan (1993). An interesting conclusion of the former study is that, under certain conditions, the upward buoyancy forces may result in flow reversal of the gas stream. Owing to his mathematical model of boundary-layer type, the author did not investigate this situation of flow reversal. Desrayaud and Lauriat (2001) have examined the condensation of laminar natural convection flow of humid air in a vertical parallel-plates channel. The plates are maintained at a temperature of 5°C and the airflow inlet temperature was 25 ~ 35°C. Their numerical results show the conditions for condensation occurrence. Condensation has also been studied by Yan and Lin (2001) in the case of laminar natural convection in vertical annuli with asymmetric isothermal and wetted walls.

The authors concluded that large amount of water evaporation was obtained with higher wall temperature, but this also results in condensation closer to the inlet at the wall whose temperature is low. Salah El Din (2003) has performed a numerical investigation of the thermal and buoyancy effects on mixed convection in a vertical channel with uniform wall heat and mass fluxes. It is interesting to mention the experimental work of Yan *et al.* (1995) on the evaporative cooling of the falling liquid film through interfacial heat and mass transfer in a vertical channel. Boulama and Galanis (2004) have obtained an analytical solution for upward, fully developed, laminar, mixed convection heat and mass transfer in a vertical channel. Recently, Jang *et al.* (2005) have conducted a numerical study on mixed convection heat and mass transfer with evaporation in an inclined square duct. They have established that heat and mass transfer related with film evaporation enhance transfer rates for systems with a lower humidity or a higher wetted wall temperature.

Most of the cited studies considered situations where both heat and mass were added to the air stream, thus the main objective was liquid film cooling. Furthermore, numerical studies neglected axial diffusion of heat, momentum and chemical species. This approach results in a set of parabolic equations resolved by the marching technique (Patankar, 1980). On the other hand, the axially parabolic model is less accurate when the buoyancy forces are important and it cannot predict flow reversal. In the present study, the adopted model includes the axial diffusion terms and, therefore, the equations are elliptical in all directions. Moreover, the conditions under investigation correspond to those encountered in air humidifier, humidification-dehumidification desalination systems or air evaporative coolers, where hot air is in direct contact with cold water. In a previous paper (Ait Hammou *et al.*, 2004), the effects of simultaneous cooling and mass transfer on the downward laminar flow of humid air in an isothermal vertical channel with wet walls have been studied. It was established that, depending on the inlet conditions of the flowing humid air, mass transfer may result in film evaporation or condensation of water vapor. On the other hand, it has been shown that thermal and solutal buoyancy forces have significant effects on flow characteristics. The main objective of the present study is to investigate the effect of thermal and buoyancy forces on both upward flow (UF) and downward flow (DF). The former is of interest in counter-flow air humidifiers. This paper is an extension of a recent conference communication by the authors (2005).

2. Problem formulation

Consider a vertical channel formed by two parallel plates (Figure 1). Air enters the channel with uniform velocity U_0, temperature T_0, and relative humidity ϕ_0. The plates are maintained at the same constant temperature and wetted by thin liquid water films. Here, we consider that these films are extremely thin so that they can be treated as a boundary condition (Yan and Lin, 1990; Yan, 1992, 1993). Steady state conditions are considered and the flow is supposed to be laminar. Viscous dissipation, radiation heat transfer and other secondary effects (such as pressure work, energy transport by the inter-diffusion of species, Dufour and Soret effects) are negligible (Gebhart and Pera, 1971). Finally, the physical properties are taken to be constant except for the density in the body forces which is considered to be a linear function of temperature and mass fraction (Boussinesq approximation):

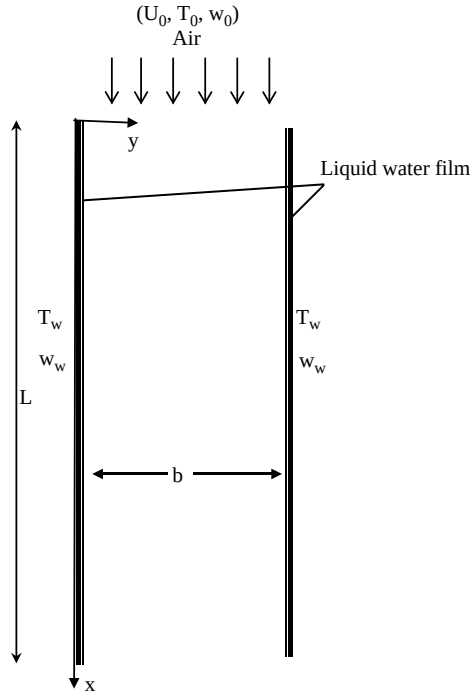

Figure 1.
Schematic representation of the physical system ($\mathbf{g} = +g\,\mathbf{x}$ in the case of a DF and $\mathbf{g} = -g\,\mathbf{x}$ in the case of an UF)

$$\rho = \rho_0[1 - \beta(T - T_0) - \beta^*(w - w_0)] \tag{1}$$

The following reference quantities are used for non-dimensionalisation: L for linear dimensions, U_0 for the velocity components, $T_w - T_0$ for the temperature difference $T - T_0$ and $w_w - w_0$ for the mass fraction difference $w - w_0$. With this formulation and the above assumptions, the governing equations of the problem can be written.

Continuity equation:

$$\frac{\partial U}{\partial X} + \frac{\partial V}{\partial Y} = 0 \tag{2}$$

Streamwise momentum equation:

$$\left(U\frac{\partial U}{\partial X} + V\frac{\partial U}{\partial Y}\right) = -\frac{\partial P_m}{\partial X} + \frac{2\gamma}{Re}\left(\frac{\partial^2 U}{\partial X^2} + \frac{\partial^2 U}{\partial Y^2}\right) \pm \frac{1}{2\gamma Re^2}(Gr_T\theta + Gr_M C) \tag{3}$$

Spanwise momentum equation:

$$\left(U\frac{\partial V}{\partial X} + V\frac{\partial V}{\partial Y}\right) = -\frac{\partial P_m}{\partial Y} + \frac{2\gamma}{Re}\left(\frac{\partial^2 V}{\partial X^2} + \frac{\partial^2 V}{\partial Y^2}\right) \tag{4}$$

Energy equation:

$$\left(U\frac{\partial\theta}{\partial X}+V\frac{\partial\theta}{\partial Y}\right)=\frac{2\gamma}{Pr\,Re}\left(\frac{\partial^2\theta}{\partial X^2}+\frac{\partial^2\theta}{\partial Y^2}\right) \tag{5}$$

Species equation:

$$\left(U\frac{\partial C}{\partial X}+V\frac{\partial C}{\partial Y}\right)=\frac{2\gamma}{Sc\,Re}\left(\frac{\partial^2 C}{\partial X^2}+\frac{\partial^2 C}{\partial Y^2}\right) \tag{6}$$

Note that in equation (3), the plus sign in front of the buoyancy term corresponds to the case of the UF and the minus sign to the case of a DF.

These equations show that six dimensionless groups define the problem: γ, Sc, Pr, Re, Gr_T and Gr_M. Instead of the Grashoff number, it is possible to consider the Richardson number, which indicates the relative intensity of the buoyancy force compared with the inertia force. Two Richardson numbers are to be considered: the thermal Richardson number $Ri_T = Gr_T/Re^2$ and the solutal Richardson number $Ri_M = Gr_M/Re^2$.

The boundary conditions for the problem under consideration are:

$$\text{At the inlet } (X=0): U=1 \text{ and } V=C=\theta=0 \tag{7}$$

$$\text{At the outlet } (X=1): \frac{\partial U}{\partial X}=\frac{\partial V}{\partial X}=\frac{\partial\theta}{\partial X}=\frac{\partial w}{\partial X}=0 \tag{8}$$

$$\text{At the walls } (Y=0 \text{ and } Y=\gamma): U=0, V=\pm V_e, C=\theta=1 \tag{9}$$

where the non-dimensional transverse velocity at the interface is (Bumeister, 1993):

$$V_e=\left(\frac{-2\gamma}{Re\,Sc}\right)(w_w-w_0)(1-w_w)^{-1}\left(\frac{\partial C}{\partial Y}\right)_{Y=0} \tag{10}$$

The mass fraction at the wall w_w corresponding to the saturation conditions at T_w, is calculated by assuming that air-vapor mixture is an ideal gas mixture.

Heat transfer between the wet wall and the humid air is the sum of a sensible and a latent component (Lee *et al.*, 1997):

$$q_T=q_S+q_L=-k\left(\frac{\partial T}{\partial y}\right)_{y=0}-\rho D h_{fg}(1-w_w)^{-1}\left(\frac{\partial w}{\partial y}\right)_{y=0} \tag{11}$$

Therefore, the Nusselt number:

$$Nu_T=\frac{hD_h}{k}=\frac{q_t D_h}{k(T_w-T_m)}=Nu_S+Nu_L \tag{12}$$

where:

$$Nu_S=-2\gamma(1-\theta_m)^{-1}\left(\frac{\partial\theta}{\partial Y}\right)_{Y=0} \tag{13a}$$

$$Nu_L = -2\gamma S(1-\theta_m)^{-1}\left(\frac{\partial C}{\partial Y}\right)_{Y=0} \tag{13b}$$

and:

$$S = \frac{\rho D h_{fg}}{k}(w_w - w_0)(1-w_w)^{-1}(T_w - T_0)^{-1} \tag{13c}$$

S represents the relative importance of energy transport through species diffusion to that through thermal diffusion.

The Sherwood number characterizes mass transfer at the interface:

$$Sh = \frac{h_M D_h}{D} = -2\gamma(1-C_m)^{-1}\left(\frac{\partial C}{\partial Y}\right)_{Y=0} \tag{14}$$

while the friction factor is:

$$fRe = 4\gamma\left(\frac{\partial U}{\partial Y}\right)_{Y=0} \tag{15}$$

3. Numerical solution

The solution of the PDEs modeling the flow field is based on the finite volume method. The velocity-pressure coupling is treated with the SIMPLER algorithm (Patankar, 1980). Convergence of this iterative procedure is declared when the relative variation of any dependent variable is less than 10^{-4} and if the mass source residual falls below 10^{-6} at all the grid points. The grid is non-uniform in both the streamwise and transverse directions with greater node density near the inlet and the walls where the gradients are expected to be more significant. To check the adequacy of the numerical scheme and the developed code the results for the case of forced heat convection were first obtained. Good agreement was found in comparison with results from the literature (Shah and London, 1978). In addition, excellent agreement was found between the present calculations and those of Yan and Lin (1989) for mixed convection heat and mass transfer. Furthermore, different grid sizes were considered to ensure that the solution was grid-independent. The details of these validations and grid sensibility study are presented in a previous work (Ait Hammou *et al.*, 2004).

4. Results and discussion

The thermophysical properties are taken to be constant and evaluated at a temperature and a concentration given by the one-third rule. This special way of evaluating the properties has been found to be appropriate for the analysis of heat and mass transfer problems (Chow and Chung, 1983; Lin *et al.*, 1988). Indeed, Chow and Chung (1983) have shown that the one-third rule works well, even at high temperature, when the stream is mostly air. The properties of air, water and their mixture are evaluated by formulas given by Fuji *et al.* (1977). All the results presented here have been calculated with an aspect ratio $L/2b = 65$.

The two Grashof numbers in equation (3) are not independent since w_w is related to T_w. So we choice T_0 and ϕ_0 as independent variables instead of Gr_T and Gr_M. Since, we are interested in studying the effect of the inlet conditions on the flow field, we have fixed the following conditions:

$$Pr = 0.7, \quad Sc = 0.58, \quad Re = 300, \quad T_w = 20°C \ (\text{hence } w_w = 14.5\,\text{g kg}^{-1}) \tag{16}$$

In light of practical situations, the selected combinations of T_0 and ϕ_0 are specified in Table I. The corresponding values of the two Grashof numbers and other relevant parameters are also indicated. Negative Grashof numbers indicate that the corresponding buoyancy force acts in the direction of gravity and so aids the entering DF or opposes the entering UF. Note that the direction of the thermal buoyancy force is the same for all the studied cases ($Gr_T < 0$). On the other hand, the direction of the solutal buoyancy force changes: it acts in the direction of gravity in cases 3 and 5 ($Gr_M < 0$) and in the opposite direction otherwise. Furthermore, the values of the thermal Richardson number are more important than those of the solutal Richardson numbers, indicating that the dominant buoyancy force here is the thermal one.

For each of the combinations of T_0 and ϕ_0 in Table I, the system of PDEs has been solved twice: once in the case of an UF and a second time in the case of a DF. The case of pure forced convection ($Gr_M = Gr_T = 0$) has also been considered for comparison purposes. By comparing the results of these numerical experiments it is possible to identify the effects of the buoyancy forces on the flow field and heat-mass transfers.

Figure 2(a) and (b) show the effect of T_0 and ϕ_0 on the axial evolution of the average air temperature, T_m, for DF and UF. We notice that the air is being cooled in all cases. In Figure 2(a), it should be noted that, at a given axial position and given T_0, T_m is lower in the case of a DF. Thus, in this kind of flow, air is being cooled more rapidly and this tendency is increased for higher values of T_0. Indeed, buoyancy forces are essentially aiding for a DF. These forces accelerate the flow and this results in an increasing of heat transfer between air and channel walls. In the case of an UF, buoyancy forces are essentially opposing and so the flow is decelerated and heat transfer decreases. A comparison of Figure 2(a) and (b) shows that the effect of T_0 is more important than that of ϕ_0. This is due to the fact that the buoyancy force induced by mass diffusion is less important than that induced by thermal diffusion (Table I).

The axial evolution of the average vapor mass fraction w_m is shown in Figure 3(a) and 3(b). In cases 1 and 4 w_m increases with x, while it decreases in cases 3 and 5.

Case No.	T_0 (°C)	ϕ_0 (percent)	w_0 (g kg^{-1})	Gr_T	Gr_M	Ri_T	Ri_M
1	40	10	4.6	−74,576	7,142	−0.8	0.08
2	40	30	13.9	−74,717	559	−0.8	0.01
3	40	50	23.3	−74,860	−6,123	−0.8	−0.07
4	45	10	6.0	−89,975	6,042	−1.0	0.07
5	70	10	19.6	−147,610	−3,045	−1.6	−0.03

Table I. Values of parameters for the studied cases

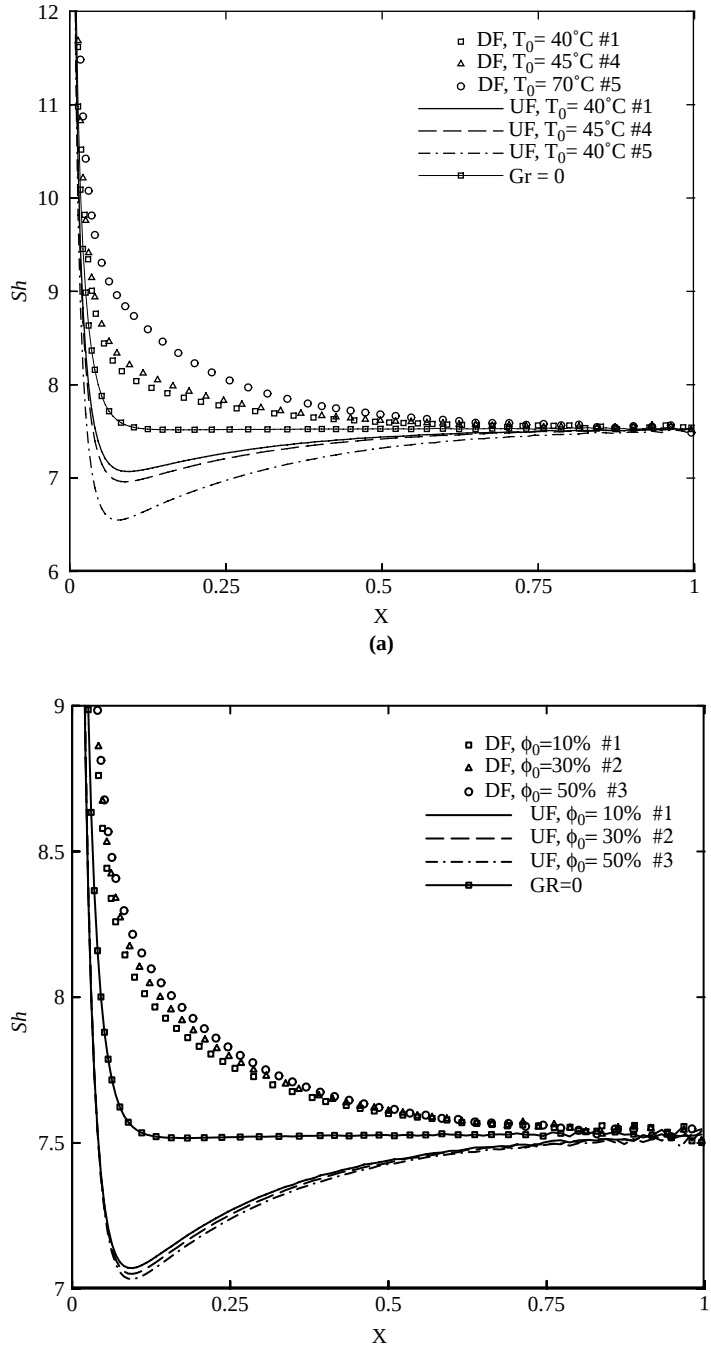

Figure 2.
Axial evolution of the average air temperature: (a) $\phi_0 = 10$ percent; (b) $T_0 = 40$°C; DF, downward flow; UF, upward flow

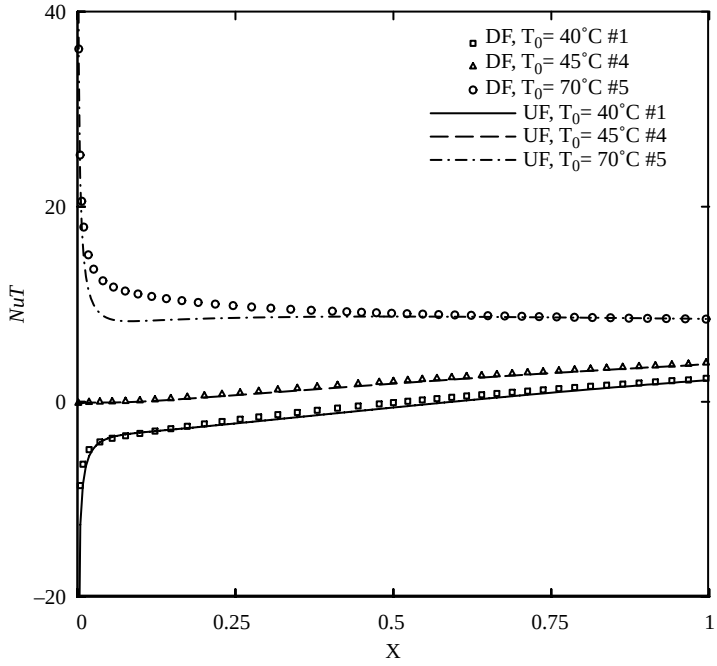

(a)

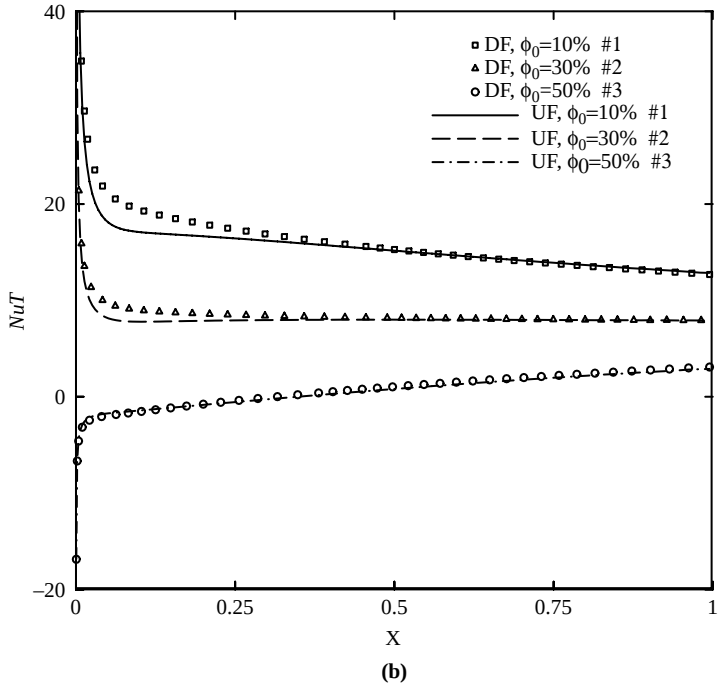

(b)

Figure 3.
Axial evolution of the average mass fraction: (a) $\phi_0 = 10$ percent; (b) $T_0 = 40$°C; DF, downward flow; UF, upward flow

In case 2, w_m stays essentially constant. In all cases, its value at the channel outlet tends towards the imposed wall condition ($w_w = 14.5\,g\ kg^{-1}$). The increase of w_m indicates that water vapor is transferred from the water film to the airflow. So evaporation of water film occurs in cases 1 and 4. While the decrease of w_m indicates that water vapor is transferred from the airflow to the water film. So condensation of water vapor takes place in cases 3 and 5. These results are consistent with the relative values of w_0 and w_w: when $w_w > w_0$ (as in cases 1 and 4) vapor flows from the liquid film to the air stream, otherwise ($w_w < w_0$ as in cases 3 and 5) it flows in the opposite direction. Finally, when $w_w \approx w_0$ (case 2) mass transfer between the wall and the fluid is negligible and w_m remains essentially constant. In cases where evaporation occurs (1 and 4, Figure 3(a)), it is noticed that at a given axial position in the entrance region, w_w is slightly more important for a DF in comparison with the upward one. On the other hand, in the cases with condensation (3 and 5, Figure 3), at a given axial position w_w is less important for a DF in comparison with the upward one. So, in both cases, the values of w_w for DF approach the final equilibrium condition earlier than for UF. This is due to the fact that the combined buoyancy force, which acts downwards in all five cases (since $Gr_T + Gr_M$ is always negative), accelerates the fluid near the wall for DF and decelerates it for UF. Therefore, near the wall more water vapor is convected downstream in the case of DF and, as a result, the corresponding dimensionless mass fraction is always lower than for UF. Hence, in light of the results in Figures 2 and 3 it is clear that air is being cooled, whether with evaporation (cases 1 and 4), with condensation (cases 3 and 5) or without mass transfer (case 2). It is believed that this situation is due to the specific conditions of the present problem, i.e. to the fact that sensible heat transfer between the warm air and the cool walls is more important than the latent heat associated with the phase change. This point will be more discussed hereafter. A recent study conducted by Marmouch *et al.* (2005) reveals a similar conclusion for analogous conditions. This study concerns heat and mass transfer in a humidifier consisting of a channel whose walls are maintained humid by a water film. It is based on one-dimensional model and takes into account the water film thickness.

The axial evolution of the friction factor is shown in Figure 4. For comparison purposes, the case of pure forced convection ($Gr_T = Gr_M = 0$) is also reported. We notice an important effect of buoyancy forces on this parameter. Also the effect of air hygrometry at the entrance is noticeable, especially the effect of T_0 (Figure 4(a)). The values of *fRe* for a DF are higher than those for pure forced convection flow. The opposite is true for an UF. These effects can be explained by examining the axial velocity profiles shown in Figure 5. This figure reveals that the axial velocity profiles are significantly modified by natural convection (i.e. buoyancy forces). The aiding buoyancy forces near the channel walls accelerate the downward airflow. This results in an increase of the velocity gradient at the wall and of the corresponding wall shear stress and friction factor (Figure 4(a)). This increase is more important as T_0 augments. Indeed, the magnitude of the buoyancy forces increases with T_0. This magnitude, given by the effective Grashof number ($Gr^+ = Gr_T + Gr_M$), is about 7×10^4 in case 1 and 15×10^4 in case 5 (Table I). It should be noted that the acceleration of the airflow near the channel walls is counterbalanced by a deceleration at the channel axis, so that the maximum velocity does not occur at the channel mid-point for a DF (Figure 5(a)). On the other hand, the opposing buoyancy

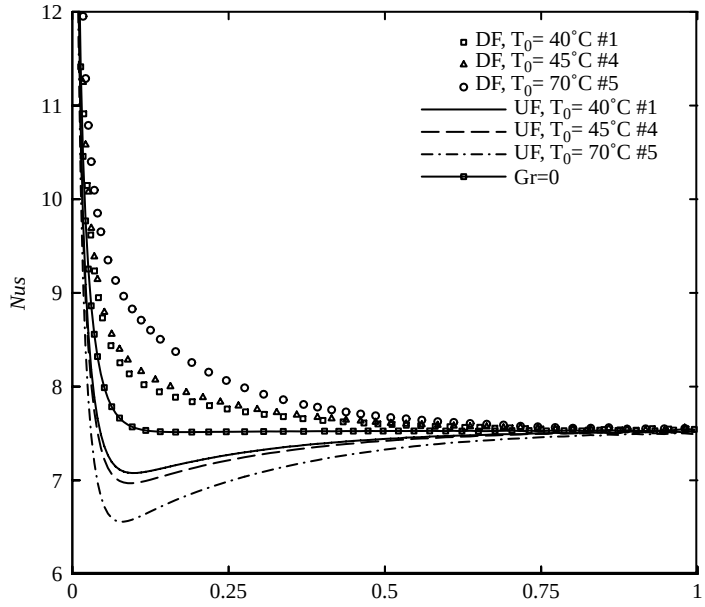

(a)

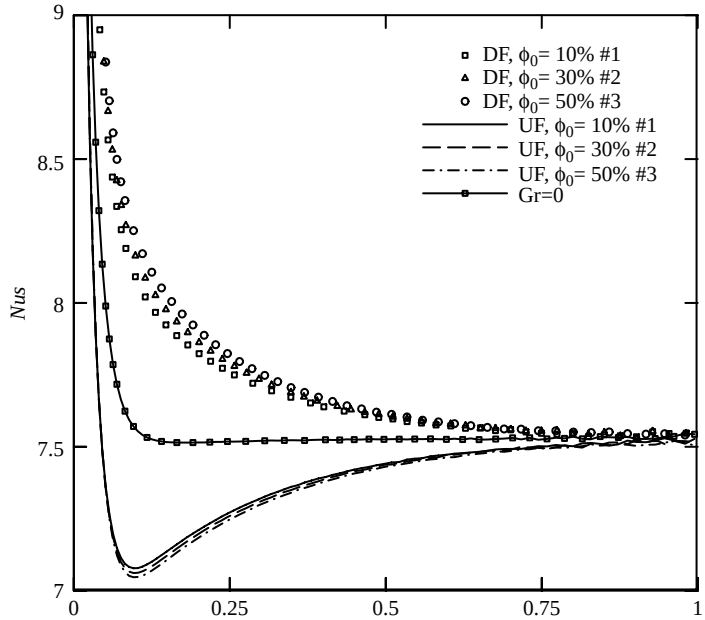

(b)

Figure 4.
Axial evolution of the friction factor: (a) $\phi_0 = 10$ percent; (b) $T_0 = 40$°C; DF, downward flow; UF, upward flow

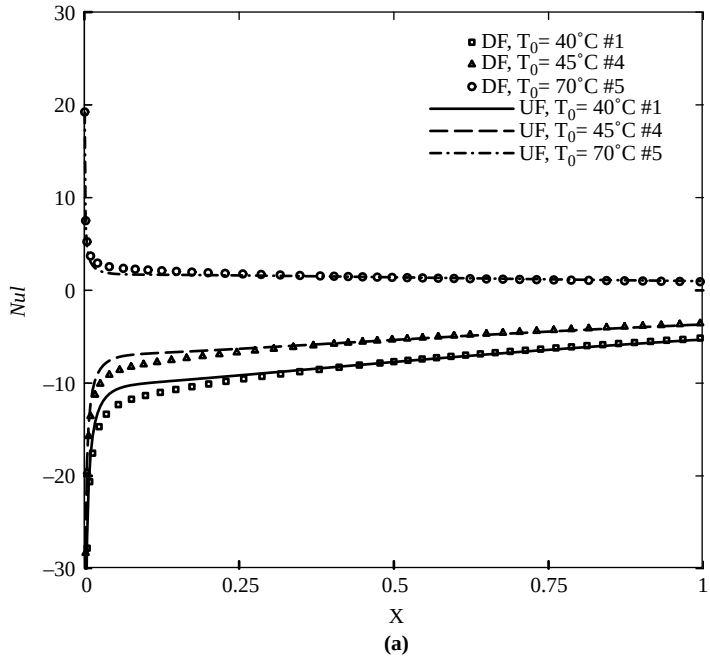

Figure 5.
Velocity profiles at $X = 0.082$: (a) $\phi_0 = 10$ percent; (b) $T_0 = 40$°C; DF, downward flow; UF, upward flow

forces near the channel walls decelerate the UF. This results in a significant decrease of *fRe* (Figure 4(a)). A careful check of this figure reveals that in case 5 *fRe* becomes negative at some axial locations. The represented velocity profiles in Figure 5(a) correspond to an axial position with $fRe < 0$. These negative values of the friction factor indicate that flow reversal occurs near the channel walls. The opposing buoyancy forces induce this flow reversal. In case 5, these forces have an important magnitude ($Gr^{+} = 15 \times 10^{4}$) so that they overcome inertia forces; this results in an axial velocity in the opposite direction of the main upward airflow (negative U in Figure 5(a)). The zone where negative values of U prevail constitutes a recirculation cell. The dimensions of this cell can be appreciated in Figure 4(a). The minimum of *fRe* in this figure corresponds to the maximum magnitude of buoyancy forces. As the airflow moves beyond this axial position, the buoyancy force becomes weaker. Thus, the inertia force pushes the air upwards and its axial velocity becomes positive, so the recirculation cell switches off.

It is important to note that Yan and Lin (1990) have mentioned this phenomenon of flow reversal in a problem similar to the present one. However, he was not able to compute it because of his boundary layer type model. Also, we mention the study of Salah El-Din (1992) and Boulama and Galanis (2004). These authors derived a criterion for flow reversal by means of an analytical study of fully developed heat and mass transfer in a vertical channel. As far as we can ascertain, the present study is the first to compute flow reversal in a developing flow with heat and mass transfer.

The axial evolution of the sensible Nusselt number is shown in Figure 6. In the case of a DF Nu_S decreases monotonically to the asymptotic value of 7.54, which corresponds to a fully developed flow (Shah and London, 1978). On the other hand, for an UF Nu_S decreases towards a minimum and then increases to the same asymptotic value. The minimum of Nu_S occurs at the same axial position as the minimum of *fRe* (Figure 4). An important effect of T_0 on Nu_S is revealed by Figure 6(a). In the case of a DF, Nu_S is higher than that for a forced convection flow and it increases with T_0. In this kind of flow, as it is shown above, buoyancy forces are aiding and their intensity increases with T_0. Thus, these forces accelerate the airflow near the channel walls (Figure 5(a)). This results in an important air temperature gradient near the walls (as it is revealed by θ vs y profiles, not shown here) and an important decrease of the mean air temperature T_m (Figure 2(a)). Thus, according to equation (13a), sensible heat transfer is increased by buoyancy forces for a DF. The opposite is true in the case of an UF where buoyancy forces are opposing for all the cases considered here. It is important to notice that differences of Nu_S between a DF and an UF are up to 38 percent in case 5.

The effect of air humidity at the entrance on Nu_S is less important than that of T_0 as we can see in Figure 6(b). However, this effect is clearer in the case of DF. Here, we can observe that Nu_S increases with ϕ_0. Indeed, increasing ϕ_0 involves a decrease in Gr_M and a small increase of Gr_T, so that the magnitude of the effective Grashof number Gr^{+} increases ($|Gr^{+}| = 67{,}434$ for $\phi_o = 10$ percent and $|Gr^{+}| = 80{,}983$ for $\phi_o = 50$ percent, see Table I). Thus, buoyancy forces, which are aiding here, increase sensible heat transfer.

Figure 7 shows the axial evolution of the latent Nusselt number. Contrary to Nu_S, the sign of Nu_L changes from negative to positive depending on the direction of the

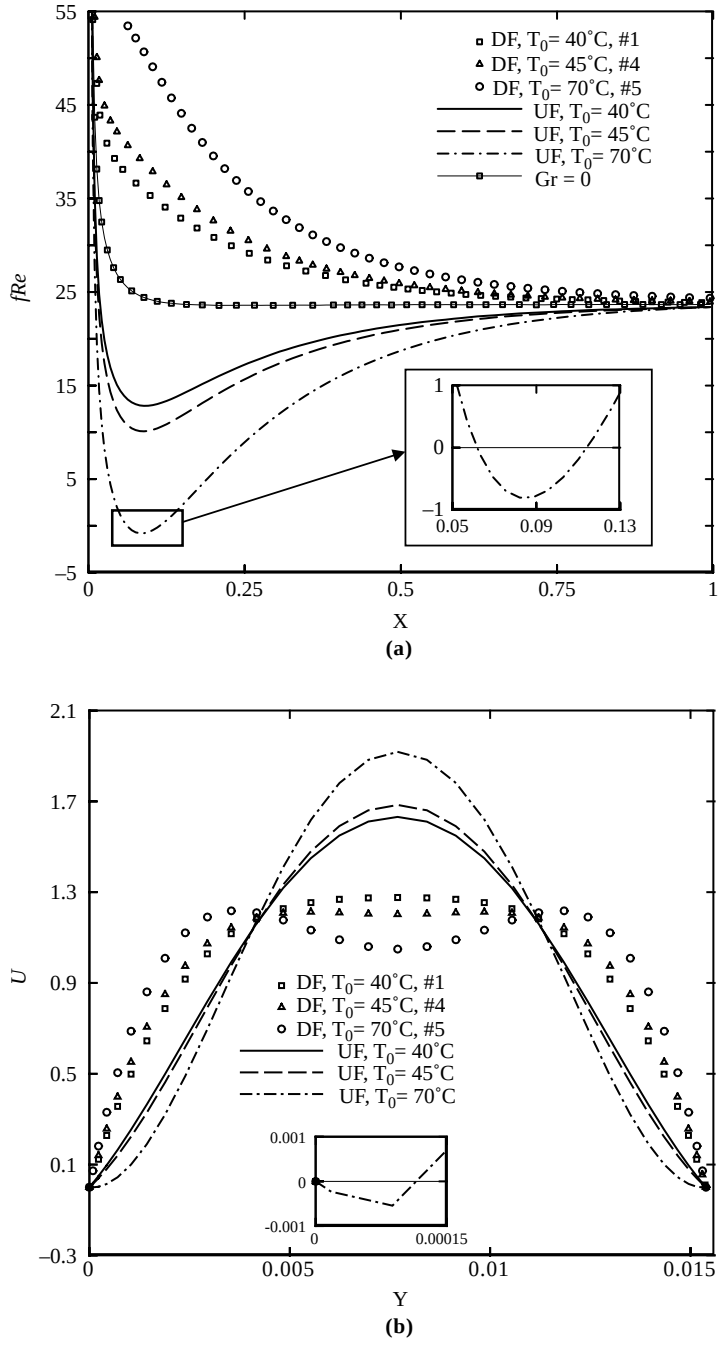

Figure 6.
Axial evolution of the sensible Nusselt number: (a) $\phi_0 = 10$ percent; (b) $T_0 = 40$°C; DF, downward flow; UF, upward flow

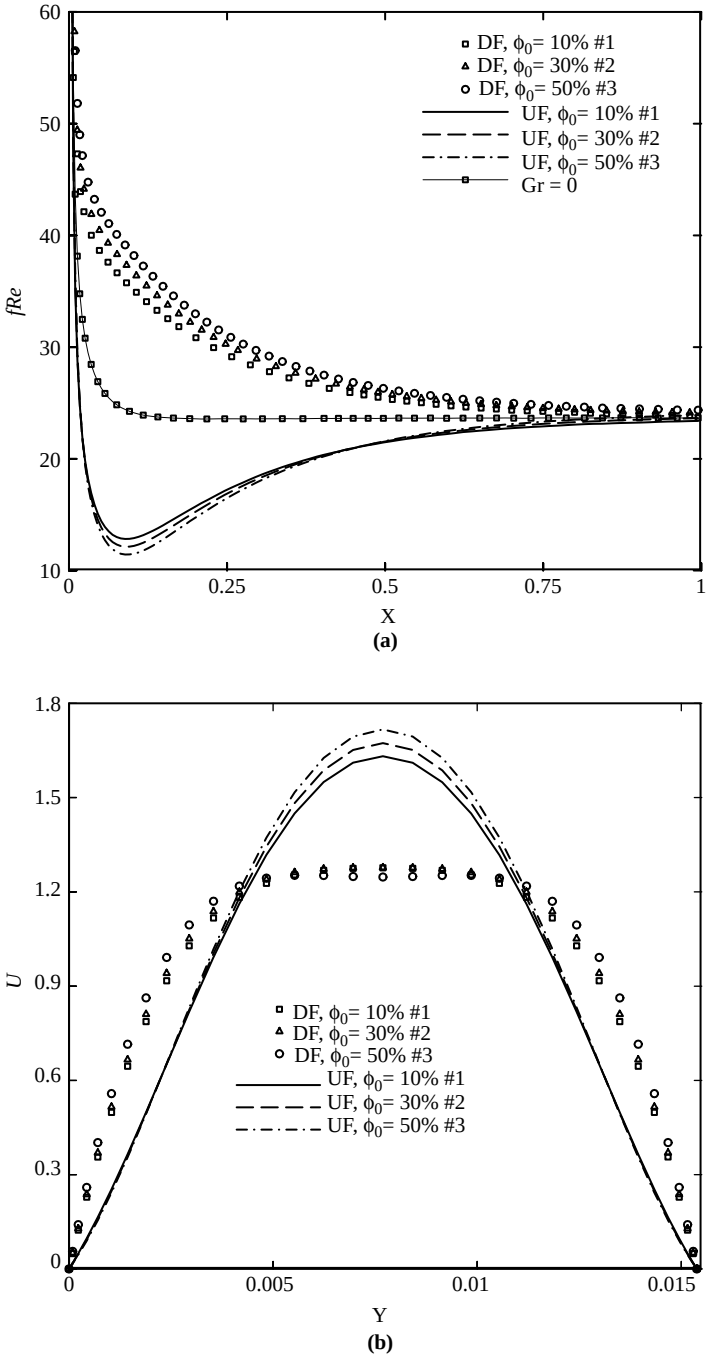

Figure 7.
Axial evolution of the latent Nusselt number: (a) $\phi_0 = 10$ percent; (b) $T_0 = 40$°C; DF, downward flow; UF, upward flow

latent heat flux. According to equations (13b) and (13c), negative Nu_L indicates that the latent heat flux is directed from the liquid film to the air ($w_w > w_0$ so there is evaporation) while positive Nu_L indicates that the latent heat flux is directed from the air to the liquid film ($w_w < w_0$ so there is condensation). It follows that in cases 1 and 4 water is evaporated and in cases 3 and 5 vapor is removed form the airflow and condensed on the film. In case 2, Nu_L is essentially zero indicating that phase change and interfacial mass transfer are negligible. Indeed, this case corresponds to $w_0 \approx w_w$ (Table I).

Figure 7 also shows that, near the channel inlet, for a given T_0 and ϕ_0, the absolute value of Nu_L is higher for a DF compared to an upward one. This effect of buoyancy forces can be explained by examining the expression of Nu_L (equation (13b)), which reveals that this effect is exerted on Nu_L by means of two parameters: the dimensionless mean temperature and the mass fraction gradient at the wall. The first parameter is higher in the case of DF because, in this case, airflow is being cooled more rapidly as it is clearly seen in Figure 2. The non-dimensional mass fraction profiles (not presented here) show that the second parameter is steeper in a DF. It is important to mention that differences of Nu_L between a DF and an UF are as high as 37 percent (case 5). These differences are of the same order as those for Nu_S.

Careful observation of Figure 7 further indicates that the difference in Nu_L between the two flow directions is negligible beyond a certain axial location which is about $X \approx 0.5$ for the studied cases. At this axial location Nu_L has the same value for the two flow directions and beyond it the absolute value of Nu_L becomes slightly more important for an UF. This inversion in Nu_L tendency is attributed to the dimensionless mass fraction gradient. It is important to mention that variations of Nu_L between a DF and an UF are up to 6 percent (case 5) for $X > 0.5$.

Another interesting effect shown in Figure 7 is that of the air hygrometry at the entrance (T_0 and ϕ_0) on the transport of latent heat associated with evaporation. As T_0 or ϕ_0 are increased, Nu_L decreases in absolute value (compare cases 1 and 4 in Figure 7(a) and cases 1 and 2 in Figure 7(b)). This trend is attributed to the S factor (see equations 13(b) and 13(c)), which diminishes in absolute value as T_0 or ϕ_0 are increased. Lee *et al.* (1997) have also reported this effect and explained it by the fact that the species diffusion mechanism is more effective at lower concentration levels. This is in agreement with our analysis considering that S factor represents the relative importance of energy transport through species diffusion to that through thermal diffusion.

The total Nusselt number Nu_T, i.e. the sum of Nu_S and Nu_L, is shown in Figure 8. An overall inspection of these figures shows that, as the airflow moves downstream, Nu_T decreases in cases 3 and 5 and increases in cases 1 and 4. These axial trends show that the minimum of Nu_S which occurs in the case of an UF (Figure 6) is not reflected in Nu_T. On the other hand, Nu_T, is positive in all cases except for case 1. At this stage, it is useful to point out the meaning of the Nusselt number signs in connection with heat flux directions. The channel walls are maintained at a temperature, which is lower than that of the airflow, so sensible heat flux is always directed towards the channel walls and Nu_S is positive. The direction of latent heat flux is the same if condensation occurs and then Nu_L is positive (cases 3 and 5 in Figure 7). If evaporation takes place, the direction of latent heat flux changes to the opposite and Nu_L is negative (cases 1 and 4, Figure 7(a)).

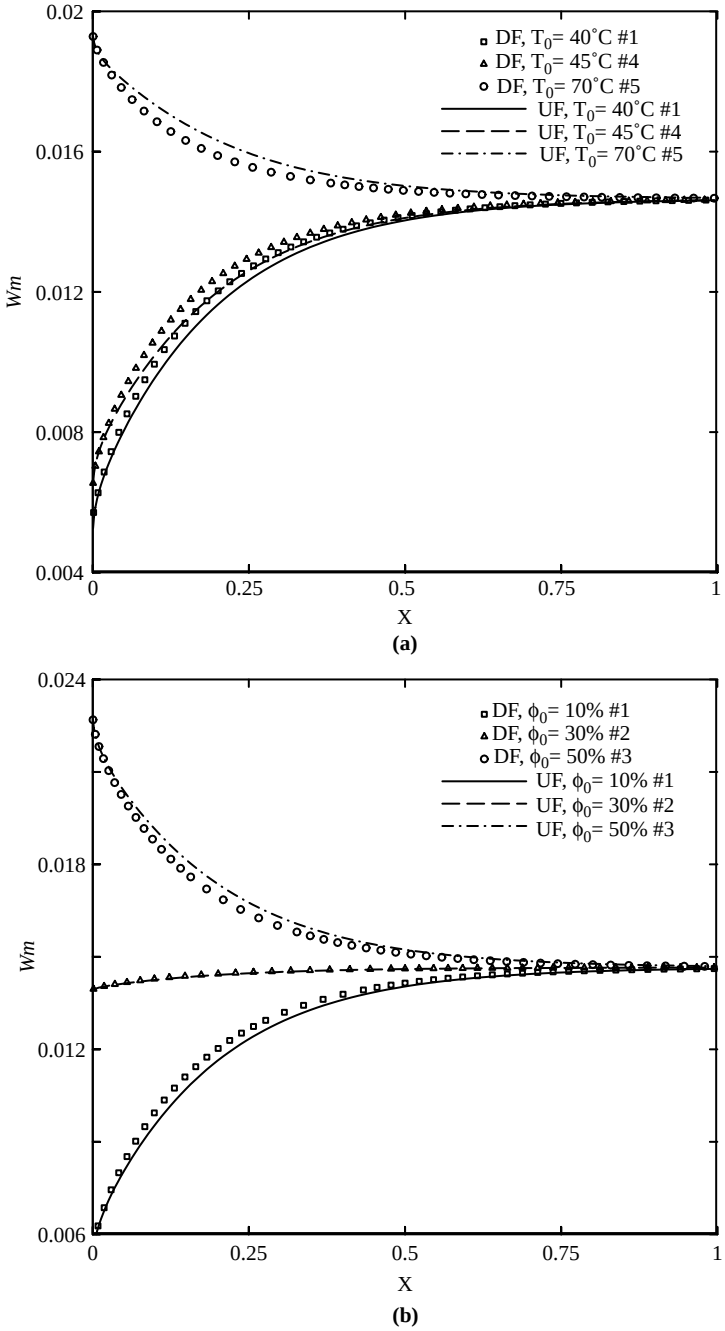

Figure 8.
Axial evolution of the total Nusselt number: (a) $\phi_0 = 10$ percent; (b) $T_0 = 40$°C; DF, downward flow; UF, upward flow

A careful inspection of Nu_T in case 1 (Figure 8(a)) leads to the following remarks about the importance of each heat flux. It is clear that, in this particular case, Nu_T is negative near the channel entrance and positive at the exit. Thus, it takes a zero value near the channel mid-point ($X \approx 0.6$). At this axial position, Nu_S and Nu_L have the same absolute value so that their sum Nu_T is zero. This feature corresponds to a situation of a zero heat balance: sensible heat flux supplied by the airflow to the channel walls is counterbalanced by latent heat flux gained by airflow by means of water film evaporation. Thus, based on the sign of Nu_T in case 1, it can be deduced that near the channel entrance Nu_L and the corresponding latent heat flux predominate (Nu_T and Nu_L have the same sign). On the other hand, beyond the channel mid-point, Nu_S and the sensible heat flux get the upper hand. In cases 2 and 4 Nu_T is positive, indicating that the sensible heat flux is predominant (Nu_L is negative in case 4 and essentially zero in case 2).

Regarding the effects of combined buoyancy forces on Nu_T in the two kinds of flow (upward and downward), and by examining the relative variations between these flows, two extreme cases are to be considered. The first is case 5 where these variations are of the same order (about 33 percent) in Nu_S, Nu_L and Nu_T. The second is case 1 where the relative variations in Nu_S and Nu_L are of the same order (about 14 percent), otherwise the variations in Nu_T are much weak (about 3 percent). In the first case (case 5), both Nu_S and Nu_L are positive, thus there is an accumulation of buoyancy effect in their sum, Nu_T. In the second case (case 1) Nu_S is positive while Nu_L is negative, thus buoyancy effects in Nu_S and Nu_L are antagonistic and so these effects are rather weak in their sum, Nu_T (Nu_T for DF and UF collapse in case 1, Figure 8).

The axial evolution of the Sherwood number, shown in Figure 9, is similar to that of Nu_S (Figure 6) as a result of the close values of the Prandtl and Schmidt numbers in this study. Overall, the buoyancy forces increase the Sherwood number (i.e. the mass transfer at the wall) in the case of a DF. For such flows, larger values of Sh are obtained for higher T_0 or ϕ_0 due to the larger combined buoyancy effects (i.e. larger values of Gr^+). On the other hand, the buoyancy forces decrease the Sherwood number in the case of an UF. For such flows, Sh decreases as T_0 or ϕ_0 increase.

5. Conclusion

The effects of natural convection on laminar heat and mass transfer between a stream of warm air and the cooler wetted walls of a vertical channel have been investigated numerically by solving the coupled elliptical partial differential conservation equations. Cases with evaporation and condensation have been investigated for both UF and DF. For the conditions under investigation, sensible heat is always directed from the air towards the walls while latent heat transfer depends on the difference between the vapor mass fraction at the channel inlet and at the walls. In four of the five investigated cases the former is more important than the latter. The results show that natural convection can increase or decrease heat and mass transfer fluxes depending on the direction of the flow. Flow reversal has been predicted for an UF with a relatively high temperature difference between the incoming air and the walls. This phenomenon is of considerable importance because it can influence flow stability and induce transition to turbulence (Tam *et al.*, 2004).

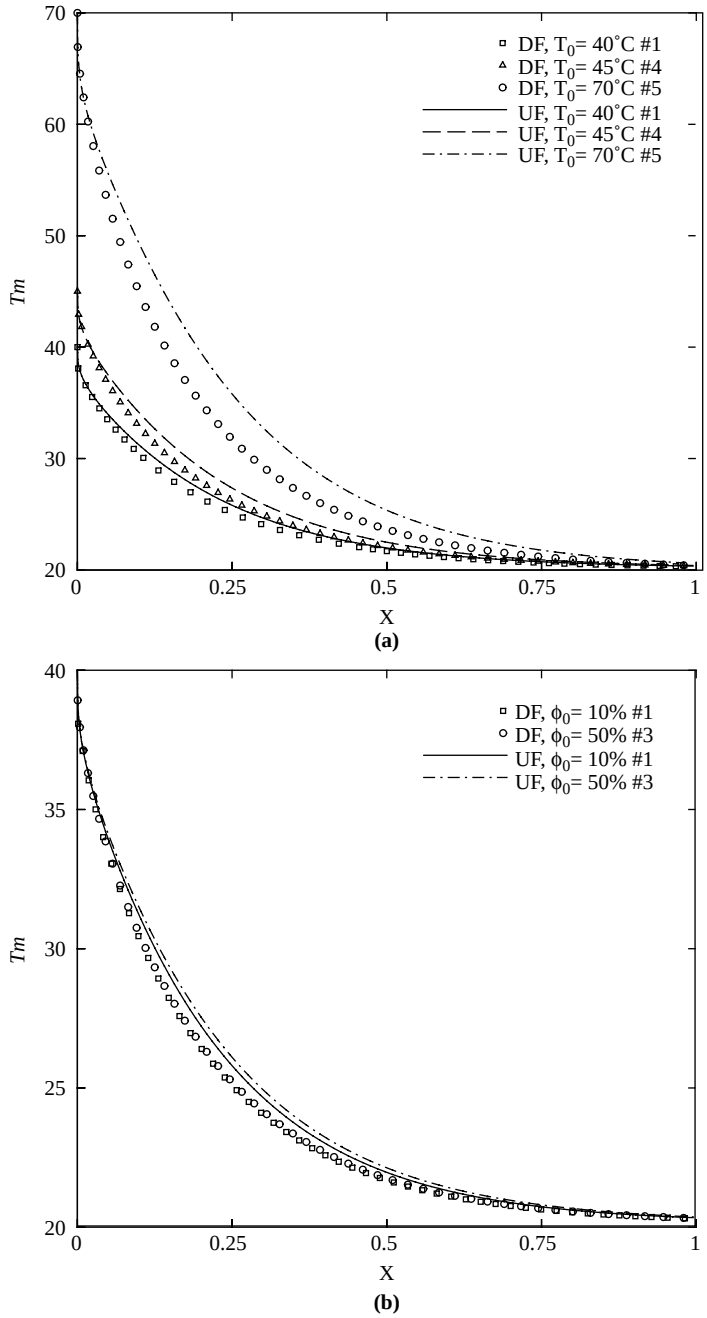

Figure 9.
Axial evolution of the Sherwood number: (a) $\phi_0 = 10$ percent; (b) $T_0 = 40$°C; DF, downward flow; UF, upward flow

References

Ait Hammou, Z., Benhamou, B., Galanis, N. and Orfi, J. (2004), "Laminar mixed convection of humid air in a vertical channel with evaporation or condensation at the wall", *Int. J. Thermal Sciences*, Vol. 43, pp. 531-9.

Boulama, K. and Galanis, N. (2004), "Analytical solution for fully developed mixed convection between parallel vertical plates with heat and mass transfer", *J. Heat Transfer*, Vol. 126, pp. 381-8.

Bumeister, L.C. (1993), *Convective Heat Transfer*, 2nd ed., McGraw-Hill, New York, NY.

Chow, L.C. and Chung, J.N. (1983), "Evaporation of water into laminar stream of air and superheated steam", *Int. J. Heat Mass Transfer*, Vol. 26, pp. 373-80.

Desrayaud, G. and Lauriat, G. (2001), "Heat and mass transfer analogy for condensation of humid air in a vertical channel", *Heat and Mass Transfer*, Vol. 37, pp. 67-76.

Fuji, T., Kato, Y. and Bihara, K. (1977), "Expressions of transport and thermodynamic properties of air, steam and water", Sei San Ka Gaku Ken Kuu Jo, Report No. 66, Kyu Shu University, Kyu Shu.

Gebhart, B. and Pera, L. (1971), "The nature of vertical natural convection flows resulting from the combined buoyancy effects of thermal and mass diffusion", *Int. J. Heat Mass Transfer*, Vol. 14, pp. 2025-50.

Jang, J.-H., Yan, W.M. and Huang, C.-C. (2005), "Mixed convection heat transfer enhancement through film evaporation in inclined square ducts", *Int. J. Heat Mass Transfer*, Vol. 48, pp. 2117-25.

Lee, K.T., Tsay, H.L. and Yan, W.M. (1997), "Mixed convection heat and mass transfer in vertical rectangular ducts", *Int. J. Heat Mass Transfer*, Vol. 40, pp. 1621-31.

Lin, T.F., Chang, C.J. and Yan, W.M. (1988), "Analysis of combined buoyancy effects of thermal and mass diffusion on laminar forced convection heat transfer in a vertical tube", *ASME J. Heat Transfer*, Vol. 110, pp. 337-44.

Marmouch, H., Benhamou, B., Orfi, J. and Ben Nasrallah, S. (2005), "Étude numérique d'un système de climatisation évaporative", 7ème Congrès de Mécanique, Casablanca, Avril 19-22.

Nelson, D.J. and Wood, B.D. (1989), "Combined heat and mass transfer natural convection between vertical parallel plates", *Int. J. Heat Mass Transfer*, Vol. 32, pp. 1779-87.

Patankar, S.V. (1980), *Numerical Heat Transfer and Fluid Flow*, Hemisphere/McGraw-Hill, New York, NY.

Salah El-Din, M.M. (1992), "Fully developed forced convection in vertical channel with combined buoyancy forces", *Int. Comm. Heat Mass Transfer*, Vol. 19, pp. 239-48.

Salah El Din, M.M. (2003), "Effect of thermal and mass buoyancy forces on the development of laminar mixed convection between parallel plates with uniform wall heat and mass fluxes", *Int. J. Thermal Sciences*, Vol. 42, pp. 447-53.

Shah, R.K. and London, A.L. (1978), *Laminar Flow Forced Convection in Ducts*, Academic Press, New York, NY.

Tam, C.T., Maiga, S.E., Landry, M., Galanis, N. and Roy, G. (2004), "Numerical investigation of flow reversal and instability in mixed laminar vertical tube flow", *Int. J. Thermal Sciences*, Vol. 43, pp. 797-808.

Yan, M.W. (1992), "Effects of film evaporation on laminar mixed convection heat and mass transfers in a vertical channel", *Int. J. Heat Mass Transfer*, Vol. 35, pp. 3419-29.

Yan, W.M. (1993), "Mixed convection heat transfer in a vertical channel with film evaporation", *Canadian J. Chemical Engineering*, Vol. 71, pp. 54-62.

Yan, W.M. and Lin, T.F. (1989), "Effects of wetted wall on laminar mixed convection in a vertical channel", *J. Thermophysics*, Vol. 3, pp. 94-6.

Yan, W.M. and Lin, T.F. (1990), "Combined heat and mass transfer in natural convection between vertical parallel plates with film evaporation", *Int. J. Heat Mass Transfer*, Vol. 33, pp. 529-41.

Yan, W.M. and Lin, D. (2001), "Natural convection heat and mass transfer in vertical annuli with film evaporation and condensation", *Int. J. Heat Mass Transfer*, Vol. 44, pp. 1143-51.

Yan, W.M., Lin, T.F. and Tsay, Y.L. (1995), "Evaporative cooling of liquid film through interfacial heat and mass transfer in a vertical channel-I. Experimental study", *Int. J. Heat Mass Transfer*, Vol. 38, pp. 2905-14.

Further reading

Azizi, Y., Benhamou, B., Galanis, N. and El-Ganaoui, M. (2005), "Heat and mass transfer in a vertical channel with phase change", *Proceedings of 4th Int. Conf. Computational Heat Mass Transfer ICCHMT, Paris, France*, May 17-20, pp. 750-5.

Corresponding author

Brahim Benhamou can be contacted at: bbenhamou@ucam.ac.ma